Journal of Zhejiang University SCIENCE
ISSN 1009-3095
http://www.zju.edu.cn/jzus
E-mail: jzus@zju.edu.cn

Design and analysis of superconducting magnets of a new mixed Maglev model*

FANG You-tong (方攸同)†1, GAO Chong-yang (高重阳)[2], YAO Ying-ying (姚缨英)[1]

([1]School of Electrical Engineering, Zhejiang University, Hangzhou 310027, China)

([2]School of Mechanical and Energy Engineering, Zhejiang University, Hangzhou 310027, China)

†E-mail: youtong@zju.edu.cn

Received Feb. 1, 2005; revision accepted Apr. 26, 2005

Abstract: A new electromagnetic suspension model using a combination of high temperature superconductors (HTS) and copper conductors is proposed in this paper. A feasibility study showed that the magnets of our model can generate the 250 kg vertical suspension force. Three dimensional FEM and Design Sensitivity Analysis using the levitation gap length and cross sectional dimensions of the HTS magnets as design parameters were conducted to obtain the optimal shape of the cross section and the configuration of the HTS magnet. It was found that the gap length when optimized HTS magnet was used was much larger than that when copper conductor magnet was used, while the HTS coil volume was minimum, and the perpendicular field along the outer surface of the HTS coil was less than 0.12 T.

Key words: HTS, Maglev, Magnet, FEM
doi:10.1631/jzus.2005.A0716 **Document code:** A **CLC number:** U266

INTRODUCTION

An electromagnetic suspension transportation system (EMS-MAGLEV) with cruising speed up to 430 km/h has been set into commercial operation in Shanghai, China since the end of 2002. This shows that research and development of EMS-MAGLEV technologies have already reached mature stage. The magnets used in the above system depicted in Fig.1 were made of copper conductors (Zhou and Siniscalchi, 2003), and its suspending gap is so small that quality requirements for track manufacturing and maintenance are very high. These disadvantages make it necessary to develop new designs of the magnet.

Wang *et al.*(2002) achieved remarkable progress in high-T_c super-conducting applications in transportation engineering. The high current density and no loss properties of super-conducting magnet allow larger levitation gap. Manufacturing cost and maintenance costs are lower for the same transportation capability. Various experimental and theoretical studies have been conducted for superconducting magnet, and a growing number of experts are trying to produce it by various approaches. Some optimal designs of high temperature superconductors (HTS) magnets in SMES and MRI were presented previously in (Noguchi *et al.*, 2002; Jo *et al.*, 2002). Common features of these designs include coreless magnets, arbitrary cross sectional shapes of HTS magnets, minimum volume of consumed HTS tape, and the anisotropic characteristic of HTS tape.

To take the advantage of the HTS concept, a new EMS-MAGLEV model with mixed HTS and copper conductor is proposed in this paper, as shown in Fig.2. With normal iron core, HTS coils fabricated by using HTS Bi-2223 for levitation and copper conductor coils for controller were selected in the design. To assess the efficiency, a 3D analysis code based on

*Project (No. 50477030) supported by the National Natural Science Foundation of China

FEM (finite element method) of reduced magnetic vector potential with Biot-Savart's law was developed. Using our approach, satisfactory solutions, as shown in the computation results, could be obtained with lower computational efforts. In addition, our Design Sensitivity Analysis yielded the optimized superconductive coil with anisotropic characteristic (J_c-B_c-T_c curve), larger gap, and smaller volume.

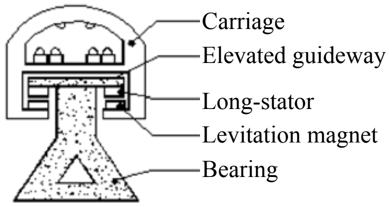

Fig.1 Suspensive and propulsive magnets in Shanghai EMS-MAGLEV commercial line

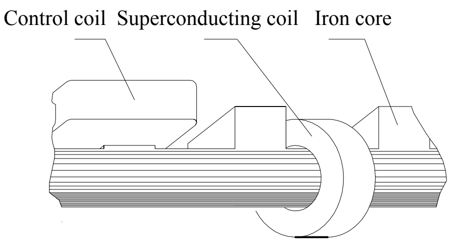

Fig.2 Hybrid EMS-MAGLEV model

In our model, because the levitating force is mainly provided by the HTS magnet, the electrical power for the same levitation will be much less than that of other designs. On the other hand, in contrast to the "full superconducting model" (Zhang *et al.*, 2004), the manufacturing of the HTS magnets in our model is much easier due to lower current frequency in the superconducting coils. However, an AC cryogenerator-free HTS magnet suffers from heat load caused by the AC loss.

3D FINITE ELEMENT ANALYSIS OF EMS-MAGLEV MAGNET

Physical model

Two typical configurations of magnets made of copper conductor coil and HTS coil, are illustrated in Figs.3a and 3b respectively, assuming that they have the same iron core. The upper iron track with slots punched in it and three-phase stator windings embedded in it is simplified as a laminated flat plate. The region containing half pole and half window in terms of the periodicity, as shown in Fig.4 where (a) is copper coil and (b) is superconducting coil, are chosen to be the 3D region for finite-element analysis.

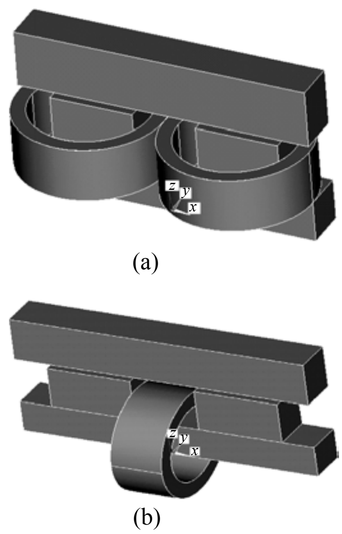

Fig.3 Structure of Maglev system magnet
(a) Copper conducting coil magnet; (b) Superconducting coil magnet

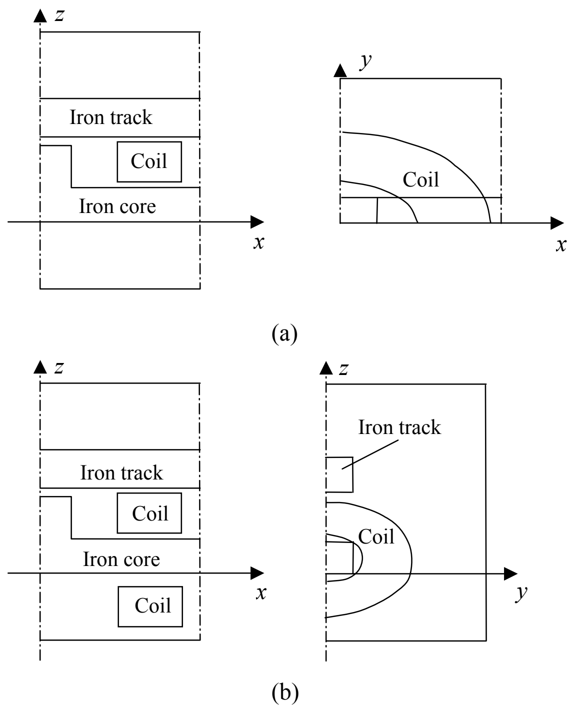

Fig.4 The 3D solving region of the investigated magnet
(a) Copper coil magnet; (b) Superconducting coil magnet

3D magnetic field formulation of reduced magnetic vector potential

The three dimensional magnetic field in space is computed by a reduced magnetic vector potential method which is effective and has many advantages (Biro and Preis, 2000). Using the method, complicated coil structures do not have to be meshed and the field caused by the coils can be calculated exactly by integration. In nuclear magnetic resonance magnet simulations, the field can be evaluated with very high accuracy because the source fields dominate and are calculated without discretization error. Total and reduced magnetic vector in the edge elements has been successfully used in the computation of the eddy currents occurring in ships (Xu and Simkin, 2004). In this work, a 3D nonlinear magnetostatic code was developed using reduced magnetic vector potential as follows.

The reduced magnetic vector potential $\boldsymbol{A}_{\mathrm{r}}$ is defined by

$$\boldsymbol{B} = \nabla \times \boldsymbol{A} = \nabla \times \boldsymbol{A}_{\mathrm{s}} + \nabla \times \boldsymbol{A}_{\mathrm{r}} = \mu_0 \boldsymbol{H}_{\mathrm{s}} + \nabla \times \boldsymbol{A}_{\mathrm{r}} \quad (1)$$

where the impressed field $\boldsymbol{H}_{\mathrm{s}}$ and the impressed vector potential $\boldsymbol{A}_{\mathrm{s}}$ describing the effect of the exciting coils can be calculated as follows by Biot-Savart law

$$\boldsymbol{A}_{\mathrm{s}} = \frac{\mu_0}{4\pi}\int_V \frac{\boldsymbol{J}_{\mathrm{s}}}{|\boldsymbol{r}-\boldsymbol{r}'|}\mathrm{d}V \quad (2)$$

$$\boldsymbol{H}_{\mathrm{s}} = \frac{1}{4\pi}\int_V \frac{\boldsymbol{J}_{\mathrm{s}} \times (\boldsymbol{r}-\boldsymbol{r}')}{|\boldsymbol{r}-\boldsymbol{r}'|^3}\mathrm{d}V \quad (3)$$

Therefore, it is possible to avoid modelling the complex sources in the finite element meshes. The governing equations for the reduced vector potential are then

$$\begin{aligned} &\nabla \times (\nu_0 \nabla \times \boldsymbol{A}_{\mathrm{r}}) - \nabla(\nu_0 \nabla \cdot \boldsymbol{A}_{\mathrm{r}}) = 0 \in \Omega_{\mathrm{air}} \\ &\nabla \times (\nu \nabla \times \boldsymbol{A}_{\mathrm{r}}) - \nabla(\nu \nabla \cdot \boldsymbol{A}_{\mathrm{r}}) = -\nabla \times (\nu \mu_0 \boldsymbol{H}_{\mathrm{s}}) \in \Omega_{\mathrm{iron}} \end{aligned} \quad (4)$$

Applying the Galerkin method to the differential equations in Eq.(4) and considering the continuity of the interface field yield the following equation:

$$\begin{aligned} &\int_{\Omega_{\mathrm{air}}} \left(\nu_0 \nabla \times \boldsymbol{A}_{\mathrm{r}} \cdot \nabla \times \boldsymbol{N} + \nu_0 \nabla \cdot \boldsymbol{A}_{\mathrm{r}} \nabla \cdot \boldsymbol{N}\right)\mathrm{d}\Omega \\ &+\int_{\Omega_{\mathrm{iron}}} \left(\nu \nabla \times \boldsymbol{A}_{\mathrm{r}} \cdot \nabla \times \boldsymbol{N} + \nu \nabla \cdot \boldsymbol{A}_{\mathrm{r}} \nabla \cdot \boldsymbol{N}\right)\mathrm{d}\Omega \\ &-\int_{\Gamma_{\mathrm{ai}}} \left(\nu_0 \nabla \times \boldsymbol{A}_{\mathrm{s}} \times \boldsymbol{n}\right) \cdot \boldsymbol{N}\mathrm{d}s = -\int_{\Omega_{\mathrm{iron}}} \left(\nu \nabla \times \boldsymbol{A}_{\mathrm{s}} \cdot \nabla \times \boldsymbol{N}\right)\mathrm{d}\nu \end{aligned} \quad (5)$$

where Γ_{ai} is the interface between Ω_{air} and Ω_{iron}, $\boldsymbol{n}$ is the outer normal of Ω_{iron}, $\boldsymbol{N}$ is the weighting function, and ν denotes the reluctivity of the field.

Optimal design of superconducting coil

With iron core, iron track and average magnetic flux density in the air gap being the same as those of the copper coil magnet, the superconducting magnet is designed to minimize cost and maximize air gap. In the optimization process, the air gap length δ and cross sectional dimensions r and z of the HTS coil in Fig.5 are chosen as the design parameters. The mathematical problem can be expressed as follows:

$$\begin{aligned} &\min\ F_{\mathrm{obj}} = \pi r z(2r_0 + r) \\ &\text{sub. to}\ \max\{B_{\perp j}\} \le 0.12\ \mathrm{T} \qquad j=1,2,\ldots,m \\ &p_i^{\mathrm{D}} \le p_i \le p_i^{\mathrm{U}} \qquad i=1,2,\ldots,n \end{aligned} \quad (6)$$

where the objective function F_{obj} stands for the volume of HTS coils; p_i^{D} and p_i^{U} are the lower and upper bounds of the design variable, respectively; p_i, r and z are the radial thickness and axial half height of the coi; r_0 is the inner radii of the coil; and $B_{\perp j}$ is the perpendicular field of the jth point on the tape flat surface of the HTS coil.

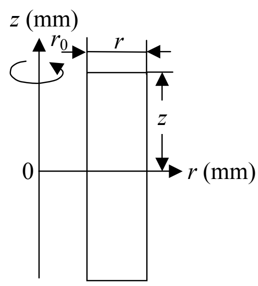

Fig.5 The cross sectional dimensions of HTS coil

Fig.6 shows the anisotropic characteristics of the I_{c}(35 K)/I_{c}(77 K) curves of Bi-2223 HTS tape. In the design, it is desired that the maximal value of perpendicular fields is kept at less than 0.12 T. Here "perpendicular fields" refer to the magnetic flux penetrating through the tape flat surface, in contrast to the "parallel field" which represents the magnetic flux parallel to the same surface.

The width and thickness of consumed HTS Bi-2223 tape were 0.25 mm and 4 mm respectively (including the thickness of insulation layers), and so, $z \geq 2$ mm, $r \geq 0.25$ mm. The exciting current in HTS coil is 10.5×880 AT.

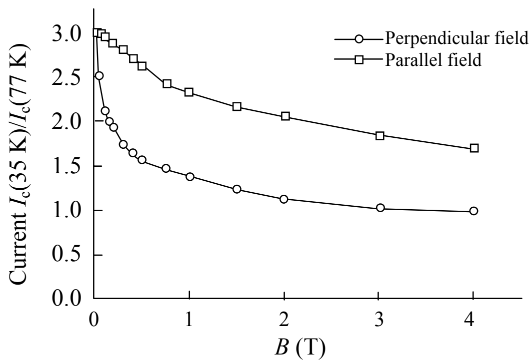

Fig.6 The I_c-B_c curves of Bi-2223 HTS tape

Design Sensitivity Analysis was successfully applied to different kinds of 3D shape optimization problems (Yao *et al.*, 2004a; 2004b; 2004c). Utilizing the normal FE analysis results, the calculation of the adjoint variable was carried out only once. With the help of the adjoint variable, design sensitivity of the objective function with respect to the design variables can be obtained easily. The required computation increases very little as the number of design variables increases. The topologically constant mesh regeneration method based on the deformation theory of the elastic body makes it possible to integrate geometric modeling, finite element mesh regenerator and optimization algorithms into a universal system to achieve optimal design automatically. In this paper, $\boldsymbol{A}_r$ method is incorporated into the above optimal design scheme to search for the preferable shape of the HTS coil.

OPTIMAL DESIGN RESULTS OF THE EMS-MAGLEV MODEL

The magnetic field of normal EMS magnet shown in Fig.2 was calculated in both 2D and 3D. The cross sections of its pole and iron core were (130 mm×130 mm) and (65 mm×130 mm), respectively. The half width and height of iron core window were 50 mm and 85 mm respectively. The air gap length δ was set to 10 mm, and the thickness of upper iron track was set to 130 mm. The copper coil exciting current was 25×270 AT. The flux linkage distributed on the symmetric surfaces is shown in Fig.7. The average flux density in the air gap was 0.696 T for 3D computation and 0.857 T for the case of 2D. The magnetic field of this kind of magnet should be computed by 3D code due to the prominent fringe effects. Then, with the same iron core, the suspensive magnet in our mixed Maglev system was designed by using Design Sensitivity Analysis. The optimized dimensions and parameters are listed in Table 1. Fig.8 and Fig.9 illustrate the magnetic field distributions on the symmetrical surfaces during the optimization, respectively. Fig.10 and Fig.11 show the perpendicular fields ($B_\perp$) distributed in a partial region of the HTS coil magnet. It is obvious that the maximum of the perpendicular fields is less than 0.12 T.

CONCLUSION

A novel strategy is presented in this paper for analyzing the static magnetic field of the Maglev sys-

Table 1 Parameters of designed HTS coil

Item	Data
Levitation gap length (mm)	14.0
Inner, outer radii and Height of HTS coil (mm)	83, 138, 16
Rated DC current and turns in HTS coil (A, Turn)	10.5, 880
Pole width×Pole length (mm^2)	130×130
Core width×Core height (mm^2)	130×65

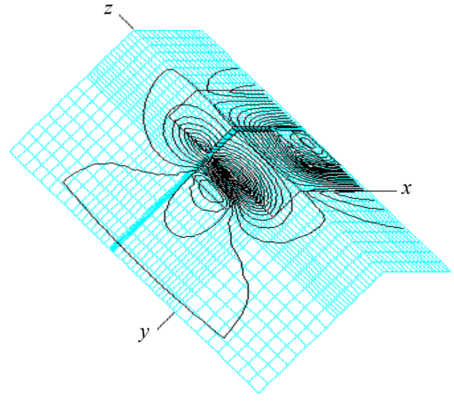

Fig.7 The flux linkage distributed on the symmetric surfaces of the copper coil magnet

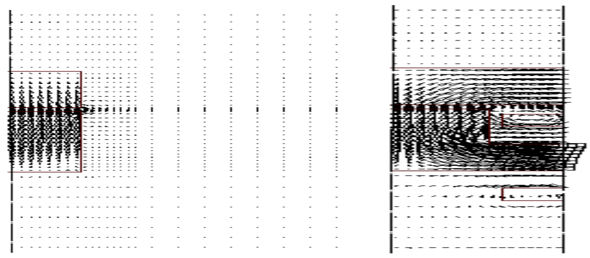

(a) (b)

Fig.8 The flux density distributed on the symmetric surfaces of the HTS coil magnet
(a) x=0; (b) y=0

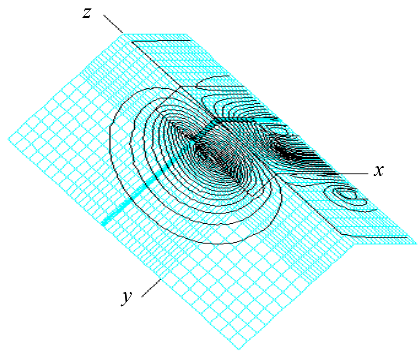

Fig.9 The flux linkage distributed on the symmetric surfaces of the HTS coil magnet

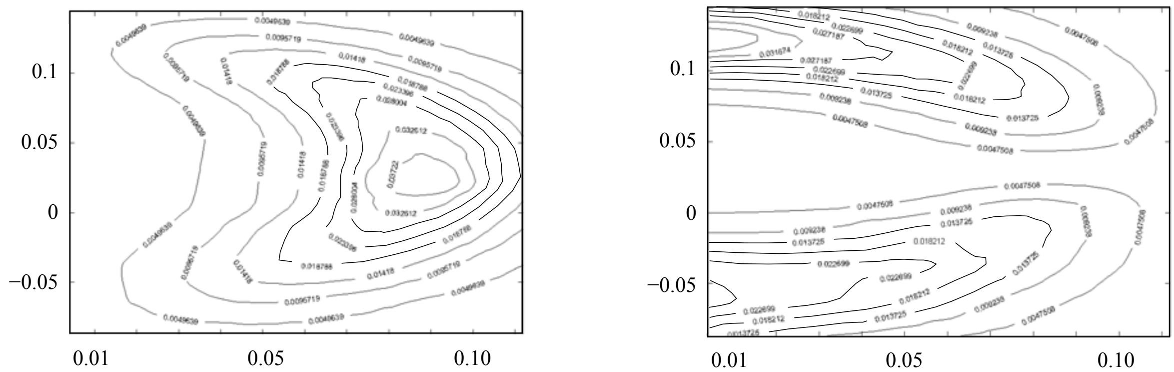

(a) (b)

Fig.10 The contour of flux density components distributed in the partial region of *yoz* surface in Fig.3b. (a) *By* contour; (b) *Bz* contour

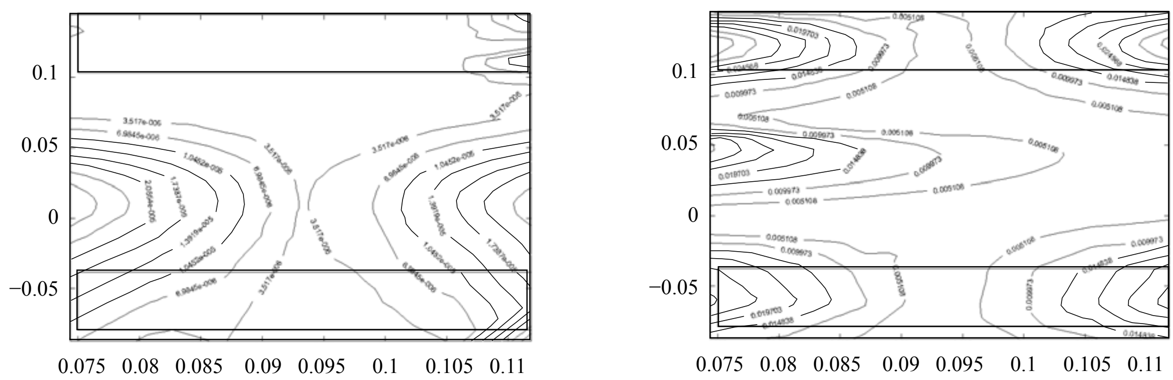

(a) (b)

Fig.11 The contour of flux density components distributed in the partial region of *xoz* surface in Fig.3b. (a) *By* contour; (b) *Bz* contour

tems magnet. The 3D magnetic fields were computed by utilizing reduced magnetic vector potential. With the help of Biot-Savart's law, the magnetic field generated by the coils can be easily calculated. Due to its smaller volume and larger suspending gap, the proposed HTS magnet designed for the mixed Maglev system is preferable to that of the EMS-MAGLEV model.

ACKNOWLEDGEMENT

The authors would like to thank Prof. Li-Sheng Wang from National Taiwan University for his very helpful comments.

References

Biro, O., Preis, K., 2000. An edge finite element eddy current formulation using a reduced magnetic and a current vector potential. *IEEE Trans. on Magnetics*, **36**(5):3128-3130.

Jo, Y., Kwon, Y., Kim, Y., Hong, J., 2002. Design of high temperature superconducting magnet. *IEEE Trans. Appl. Superconduct*., **12**(1):721-724.

Noguchi, S., Yamashita, H., Ishiyama, A., 2002. An optimal design method for SMES coils using HTS tape. *IEEE Trans. Appl. Superconduct*., **12**(1):1459-1462.

Wang, J.S., Wang, S.Y., Ren, Z.Y., Jiang, H., Zhu, M., Wang, X.R., Shen, X.M., Song, H.H., 2002. Experimental Results of High Temperature Superconducting Maglev Vehicle. Superconductors for Practical Applications (SPA'2002), Xi'an, China.

Xu, E., Simkin, J., 2004. Total and reduced magnetic vector potentials and electrical scalar potential for eddy current calculation. *IEEE Trans. on Magnetics*, **40**(2):938-940.

Yao, Y., Ryu, J.S., Koh, C.S., Xie, D., 2004a. Utilizing design sensitivity analysis for 3D optimization of transformer tank shields considering eddy current. *COMPEL*, **23**(2):506-517.

Yao, Y., Ryu, J.S., Koh, C.S., Xie, D., 2004b. 3D optimal shape design of magnetic pole in permanent magnet assembly for MRI taking account of eddy current. *IEEE Trans. on Magnetics*, **40**(2):1164-1167.

Yao, Y., Ryu, J.S., Koh, C.S., Xie, D., 2004c. A novel mesh regeneration using structural deformation analysis for 3D shape optimization of electromagnetic devices. *IEEE Trans. on Magnetics*, **40**(2):1009-1012.

Zhang, G., Fang, Y., Song, F., Zhu, G., Wang, Z., 2004. Optimal design and FEM analysis of the superconducting magnets of EMS-MAGLEV models using Bi-2223 tapes. *IEEE Trans. on Appl. Superconduct*., **14**(2):1850-1853.

Zhou, W., Siniscalchi, G., 2003. EMS-MAGLEV train took off from Shanghai. *Newton Magazine*, (2):6-12 (in Chinese).